

Preparation and Characterization of Palladium Shells with Gold and Silica Cores

Jun-Hyun Kim, Hae-Won Chung, and T. Randall Lee*

Department of Chemistry, University of Houston, 4800 Calhoun Road, Houston, Texas 77204-5003

Received December 31, 2005. Revised Manuscript Received May 16, 2006

This paper describes the structural and optical properties of core–shell particles in which the outer shell is composed of palladium and the inner core is composed of either gold (conducting) or silica (dielectric). Monodispersed gold-core particles having ~ 75 nm diameters were prepared by conventional citrate reduction; silica-core particles having diameters ranging from 100 to 500 nm were prepared by the Stöber method. The silica-core particles were functionalized with amine groups and seeded with small gold nanoparticles (~ 2 – 3 nm). Both types of core particles were then coated with palladium to afford controllable sizes of core–shell particles ranging from ~ 100 to 600 nm in overall diameter (i.e., the palladium shell thickness could be varied from 10 to 60 nm). The optical properties, morphology, and elemental composition of the composite nanoparticles were characterized by UV–vis, FE-SEM, EDX, DLS, and TEM. The results demonstrate that palladium shell nanoparticles can be reliably prepared in a controlled fashion and that their optical absorptions are broadened and shifted to longer wavelength compared to simple palladium nanoparticles.

Introduction

A variety of preparative methods have been explored in efforts to produce spherical metallic nanoparticles composed of gold, silver, platinum, and palladium.^{1–4} Nanoscale palladium particles have drawn particular attention due to their catalytic and magnetic properties.^{5–8} The use of palladium nanoparticles in catalysis is not only industrially important (e.g., automobile catalytic converters and various hydrogenation reactions)^{9–12} but also scientifically interesting, given the sensitive relationship between catalytic activity and nanoparticle size and shape as well as the nature of the surrounding media.^{13,14}

Palladium nanoparticles can be readily produced via solution thermolysis,^{15,16} sonochemical methods,¹⁷ electro-

chemical methods,¹⁸ and radiolysis.^{19,20} To prevent particle aggregation, most routes often involve metal ion reduction in the presence of heterogeneous supports or stabilizers, including electrode surfaces and organic molecules, polymers, or surfactants. Little work, however, has so far been able to produce discrete palladium nanoparticles having uniformly large sizes (e.g., ≥ 50 nm).²¹ In contrast to the aforementioned approaches, we believed that a core–shell strategy²² might allow the controlled preparation of palladium particles without requiring external stabilizers.²³

Other research has explored bimetallic gold–palladium nanoparticles for use in catalysis.²⁴ Studies of catalytic olefin hydrogenation found that the activity of bimetallic gold–palladium nanoparticles was greater than that of corresponding mixtures of gold and palladium monometallic nanoparticles. Furthermore, gold nanoparticles not only are biocompatible but also possess unique optical properties, including a strong plasmon absorption, which offers unique opportunities in bio-nano engineering.^{25–30} Much of the work in this

- (1) Chow, M. K.; Zukoski, C. F. *J. Colloid Interface Sci.* **1994**, *165*, 97.
- (2) Bright, R. M.; Musick, M. D.; Natan, M. J. *Langmuir* **1998**, *14*, 5695.
- (3) Petroski, J. M.; Wang, Z. L.; Green, T. C.; El-Sayed, M. A. *J. Phys. Chem. B* **1998**, *102*, 3316.
- (4) Ye, H.; Scott, R. W. J.; Crooks, R. M. *Langmuir* **2004**, *20*, 2915.
- (5) Esumi, K.; Isono, R.; Yoshimura, T. *Langmuir* **2004**, *20*, 237.
- (6) Teranshishii, T.; Miyake, M. *Chem. Mater.* **1999**, *11*, 3414.
- (7) Haberland, H., Ed. *Clusters of Atoms and Molecules*; Springer-Verlag: New York, 1994.
- (8) Turton, R. *The Quantum Dot: A Journey into the Future of Microelectronics*, Oxford University: New York, 1995.
- (9) Hirai, H.; Toshima, N. *Tailored Metal Catalysts*; Iwasawa, Y., Ed.; D. Reidel: Dordrecht, 1986.
- (10) Toshima, N.; Wang, Y. *Adv. Mater.* **1994**, *6*, 245.
- (11) Bard, A. J. *Science* **1980**, *207*, 139.
- (12) Willner, I.; Mairan, R.; Mandler, D.; Dürr, H.; Dörr, G.; Zengerle, K. *J. Am. Chem. Soc.* **1987**, *109*, 6080.
- (13) Mizukoshi, Y.; Okitsu, K.; Maeda, Y.; Yamamoto, T. A.; Oshima, R.; Nagata, Y. *J. Phys. Chem. B* **1997**, *101*, 7033.
- (14) Giorgio, S.; Chapon, C.; Henry, C. R. *Langmuir* **1997**, *13*, 2279.
- (15) Lee, C.-H.; Huang, Y.-C.; Wan, C.-C.; Wang, Y.-Y.; Ju, Y.-J.; Kuo, L.-C.; Oung, J.-C. *J. Electrochem. Soc.* **2005**, *152*, C520.
- (16) Teranishi, T.; Miyake, M. *Chem. Mater.* **1998**, *10*, 594.
- (17) Nemamcha, A.; Rehspringer, J.-L.; Khatmi, D. *J. Phys. Chem. B* **2006**, *110*, 383.

- (18) Zhang, P.; Sham, T. K. *Appl. Phys. Lett.* **2003**, *82*, 1778.
- (19) Michaelis, M.; Henglein, A. *J. Phys. Chem.* **1992**, *96*, 4719.
- (20) Sarkany, A.; Papp, Z.; Sajo, I.; Schay, Z. *Solid State Ionics* **2004**, *176*, 209.
- (21) For a notable exception, see: Lu, L.; Wang, H.; Xi, S.; Zhang, H. *J. Mater. Chem.* **2002**, *12*, 156.
- (22) Remita, H.; Etcheberry, A.; Belloni, J. *J. Phys. Chem. B* **2003**, *107*, 31.
- (23) Colvin, V. L.; Schlamp, M. C.; Alivisatos, A. P. *Nature* **1994**, *370*, 354.
- (24) See, for example: Harada, M.; Asakura, K.; Toshima, N. *J. Phys. Chem. B* **1993**, *97*, 5103.
- (25) Logunov, S. L.; Ahmadi, T. S.; El-Sayed, M. A.; Khoury, J. T.; Whetten, R. L. *J. Phys. Chem. B* **1997**, *101*, 3713.
- (26) Zhu, M. Q.; Wang, L. Q.; Exarhos, G. J.; Li, A. D. Q. *J. Am. Chem. Soc.* **2004**, *126*, 2656.
- (27) Aden, A. L.; Kerker, M. *J. Appl. Phys.* **1951**, *22*, 1242.
- (28) Oldenburg, S. J.; Jackson, J. B.; Westcott, S. L.; Halas, N. J. *Appl. Phys. Lett.* **1999**, *75*, 2897.

area, however, has been restricted to gold-shell silica-core nanoparticles as well as the related silver-shell silica-core nanoparticles.^{31,32} One of the major advantages of the silica-core nanoparticles is that the cores can be grown with low polydispersities (e.g., <1%).³³ Silica particles are also optically transparent and can be readily patterned on a variety of surfaces.^{34,35}

In contrast to the studies of gold-shell and silver-shell nanoparticles, the goal of this work was to prepare and study palladium-shell nanoparticles having various core types and sizes. We anticipate the ability to use UV, visible, and near-infrared light to enhance the catalytic activity of these nanoparticles via activation of the palladium surface plasmon. To this end, we report here that palladium shells with both nonconducting silica cores and conducting gold cores can be reproducibly prepared in sizes ranging from ~100 to 600 nm in diameter without requiring the use of external stabilizers. Furthermore, due to the absence of strongly bound surface-adsorbed species, it is likely that these nanoparticles can be readily modified for further applications through the use of self-assembled monolayer (SAM) technology.^{36,37}

Experimental Section

Materials. All reagents (except for water) were purchased from the indicated suppliers and used without modification. Ammonium hydroxide (30% NH₃), trisodium citrate dihydrate, nitric acid, hydrochloric acid (all from EM Science), tetraethyl orthosilicate (TEOS), 3-aminopropyltrimethoxysilane (APTMS), tetrakis(hydroxymethyl)phosphonium chloride (THPC, all from Aldrich), hydrogen tetrachloroaurate(III) hydrate (Strem), ethanol (McKormick Distilling Co.), potassium carbonate (J. T. Baker), palladium(II) chloride (Acros), and L-ascorbic acid sodium salt (Chemalog). Deionized water was purified to a resistance of 18 M Ω (Academic Milli-Q Water System, Millipore Corporation) and filtered through a 0.22 μ m filter membrane to remove any impurities. All glassware and equipment used in the experiments were cleaned in aqua regia solution (3:1, HCl:HNO₃) followed by cleaning in a base bath (saturated KOH in isopropyl alcohol) and rinsing in Milli-Q water prior to use.

Preparation of Gold and Amine-Functionalized Silica Particles. Bare gold nanoparticles were prepared via the common technique of citrate reduction, which has been described in detail elsewhere.^{38–40} The average diameter of our gold nanoparticles was always between 70 and 80 nm as judged by FE-SEM, TEM, and DLS.

The preparation of amine-functionalized silica nanoparticles involves a slight modification of the well-known Stöber method for preparing 95–100 nm silica-core nanoparticles.³³ An aliquot (12 mL, 300 mmol) of ammonium hydroxide was added to 200 mL of absolute ethanol in a 500 mL two-necked round-bottomed flask. The mixture was stirred for 30 min at 30 °C. An aliquot (6.8 mL, 31 mmol) of tetraethyl orthosilicate (TEOS) was rapidly added to the mixture. The solution changed from colorless to milky white in ~30 min, and stirring was continued overnight. An excess (0.25 mL, 1.4 mmol) of aminopropyltrimethoxysilane (APTMS) was then added to the solution.⁴¹ The mixture was vigorously stirred for another 6–8 h and heated to 88 °C for another 1 h to promote covalent bonding of the APTMS moieties onto the silica particles.⁴² Approximately 10 mL of ethanol was added dropwise during refluxing to maintain the volume of the solution. The amine-functionalized silica particles were centrifuged using a RC-3B Refrigerated Centrifuge (Sorvall Instruments) at 2500 rpm for 1 h. The particles were twice redispersed in 200 mL of ethanol to remove unattached APTMS and small silica nanoparticle contaminants.

Attachment of THPC Gold Seeds to Amine-Functionalized Silica Particles. This procedure involved a modification of the Westcott et al. method for attaching gold-seed particles on silica-core particles.⁴³ The gold-seed solution was prepared via modification of the Duff et al. method.^{44,45} First, 1 mL of a 1 M solution of NaOH, 2 mL of THPC solution (12 μ L of 80% THPC in 1 mL of water), and 200 mL of Milli-Q water were mixed in a 250 mL flask and vigorously stirred for at least 15 min. An aliquot (4 mL) of 1% aqueous HAuCl₄·H₂O was added quickly to the stirred solution, which was stirred further for ~30 min. The color of the solution changed very quickly from colorless to dark reddish yellow, which we call “THPC gold nanoparticles”. Although the size of the THPC gold nanoparticles can be varied,⁴⁴ our gold seeds were consistently ~2–3 nm in diameter. The solution of THPC gold seeds was stored in the refrigerator for at least 3 days before further use. The aged THPC gold nanoparticles (50 mL) were added to the silica-core particles (1 mL); the mixture was shaken for a couple of minutes and then left overnight for self-assembly. The mixture was then centrifuged for 1 h at 3000 rpm to remove unattached THPC gold seeds. The dark red-colored precipitate was redispersed in 50 mL of water, sonicated for 5 min, and then centrifuged again for 1 h. The solution was light red in color after the final precipitate was redispersed in 50 mL of water.

Palladium Nanoshell Growth. This procedure involved a modification of the Turkevich et al. method, which is used to prepare palladium nanoparticles having diameters smaller than 45 nm.⁴⁶ A 1 mM solution of palladium chloride was prepared by dissolving 0.01773 g of PdCl₂ in a mixture of 98 mL of water and 2 mL of 50 mM of HCl solution. An aliquot (10 mL) of this solution was placed in a 25 mL beaker containing a magnetic stirring bar, and then varying amounts of THPC gold-seeded silica nanoparticles (i.e., 1 to 8 mL) were added to produce palladium shells of varying thickness.⁴⁷ For shell growth, the mixture was stirred at least 10 min, and then 1.2 mL of 100 mM L-ascorbic acid (a mild reducing agent) was added to reduce the palladium onto the core particles. The color of the solution changed from yellow to light gray, to

- (29) Oldenburg, S. J. Ph.D. Thesis, Department of Electrical Engineering, Rice University, Texas, 1999.
- (30) Ser-shen, S. R.; Westcott, S. L.; Halas, N. J.; West, J. L. *Appl. Phys. Lett.* **2002**, *80*, 4609.
- (31) Oldenburg, S. J.; Averitt, R. D.; Westcott, S. L.; Halas, N. J. *Chem. Phys. Lett.* **1998**, *288*, 243.
- (32) Jackson, J. B.; Halas, N. J. *J. Phys. Chem. B* **2001**, *105*, 2743.
- (33) Stöber, W.; Fink, A.; Bohn, E. *J. Colloid Interface Sci.* **1968**, *26*, 62.
- (34) Van Helden, A. K.; Vrij, A. *J. Colloid Interface Sci.* **1980**, *78*, 312.
- (35) Leite, C. A. P.; de Souza, E. F.; Galembek, F. *J. Braz. Chem. Soc.* **2001**, *12*, 519.
- (36) Love, J. C.; Gates, B. D.; Wolfe, D. B.; Paul, K. E.; Whitesides, G. M. *Nano Lett.* **2002**, *2*, 891.
- (37) Kim, J.-H.; Lee, T. R., manuscript in preparation.
- (38) Frens, G. *Nat. Phys. Sci.* **1973**, *241*, 20.
- (39) Turkevich, J.; Stevenson, P. C.; Hillier, J. *Discuss. Faraday Soc.* **1951**, *58*, 55.
- (40) Goodman, S. L.; Hodges, G. H.; Trejdosiewicz, L. K.; Linvinton, D. C. *J. Microsc.* **1981**, *123*, 201.

- (41) Waddell, T. G.; Leyden, D. E.; DeBello, M. T. *J. Am. Chem. Soc.* **1981**, *103*, 5303.
- (42) van Blaaderen, A.; Vrij, A. *J. Colloid Interface Sci.* **1993**, *156*, 1.
- (43) Westcott, S. L.; Oldenburg, S. J.; Lee, T. R.; Halas, N. J. *Langmuir* **1998**, *14*, 5396.
- (44) Duff, D. G.; Baiker, A. *Langmuir* **1993**, *9*, 2301.
- (45) Duff, D. G.; Baiker, A. *Langmuir* **1993**, *9*, 2310.
- (46) Turkevich, J.; Kim, G. *Science* **1970**, *169*, 873.
- (47) In the absence of THPC gold seeds on the amine-functionalized silica-nanoparticle cores, no palladium shells were observed to form.

dark gray, and/or to steel blue depending on the shell thickness. Palladium shells on gold cores were prepared in the same manner. Solutions of these latter particles are slightly brighter in color than those having silica cores. All samples were centrifuged and redispersed in Milli-Q water to remove unreacted reagents and side products. The solutions were stored in the refrigerator (4 °C) to inhibit any aggregation before analysis.

Characterization Methods. The nanoparticles were examined by ultraviolet–visible (UV–vis) spectroscopy, field emission scanning electron microscopy (FE-SEM), transmission electron microscopy (TEM), dynamic light scattering (DLS), and energy dispersive X-ray (EDX) analysis.

To evaluate the size and morphology of the particles, we employed a JSM 6330F (JEOL) FE-SEM instrument operating at 15 kV and equipped with a setup for elemental analysis by EDX (Link ISIS software series 300, Oxford Instruments). To obtain high-resolution images, all samples were placed on a carbon-coated copper grid and dried thoroughly at room temperature overnight prior to the carbon coating. The samples were then coated with carbon via sputtering to improve electrical conductivity. The samples were examined at a magnification of 20000 to 150000 to evaluate the uniformity and morphology.

Similarly, we examined particle size and morphology at high resolution using a JEM-2000 FX electron microscope (JEOL) TEM analysis at an accelerating voltage of 200 kV. All TEM samples were deposited on 300 mesh holey carbon coated-copper grids and dried overnight before analysis.

As an independent measure of particle size, we performed dynamic light scattering (DLS) measurements using an ALV-5000 Multiple Tau Digital Correlation instrument operating at a light source wavelength of 514.5 nm and a fixed scattering angle of 90°. The average diameters of all samples were evaluated (100 s, five times) and compared to the data from FE-SEM and TEM for consistency.

UV–vis spectra were obtained using a Cary 50 Scan UV–visible spectrometer over the wavelength range of 200–1100 nm. All samples were centrifuged, redispersed, diluted in Milli-Q water, and then transferred into a quartz UV cell having a path length of 1 cm.

Results and Discussion

In initial studies, we attempted to grow palladium shells by the direct reduction of palladium salts onto the surface of amine-functionalized silica particles (i.e., without using small gold seeds as nucleation sites for shell growth). Despite several attempts, these experiments led to incomplete, aggregated, and/or small palladium particles attached to the silica-core particles (data not shown). Apparently, the presence of multiple nucleation sites is required for palladium shell growth (vide infra).

We then adopted the method of seeded growth of nanoparticles to produce stable colloidal dispersions of palladium shells on silica nanoparticle cores.^{31,48} We also explored the growth of palladium shells on gold nanoparticle cores. Our studies found that both types of Pd-shell particles could be reproducibly prepared at room temperature using mild reducing agents. We do not know the precise mechanism(s) by which the palladium salts form shells on the gold nanoparticles,⁴⁹ but a previous report suggests that the process involves particle-mediated electron transfer from ascorbic acid to palladium ions.²¹ Dispersions of the composite nanoparticles in solution exhibited colors that were dependent

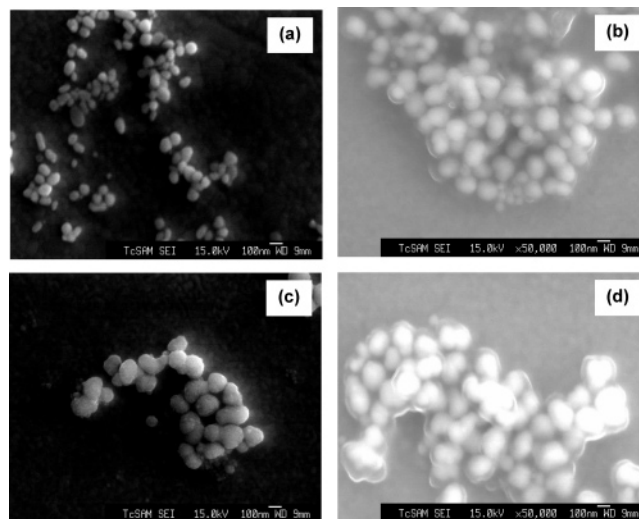


Figure 1. FE-SEM images of (a) bare gold nanoparticles ~ 75 nm in diameter and the same cores with Pd shells having thicknesses of (b) ~ 10 nm, (c) ~ 20 nm, and (d) ~ 30 nm.

on the thickness of the palladium shells. Moreover, we were able to evaluate the surface morphologies of the palladium nanoparticles (diameter range from 100 to 600 nm) using FE-SEM; in contrast to most previous studies,^{21,46} the use of FE-SEM to evaluate the morphology of palladium nanoparticles has been fruitless because the diameters of the particles are typically smaller than 50 nm.

Figure 1 shows typical FE-SEM images of bare gold and Pd-coated gold nanoparticles prepared as described in the Experimental Section. From the FE-SEM images and DLS measurements, the diameter of the bare gold nanoparticles was ~ 75 nm, while the Pd-coated gold nanoparticles could be varied from ~ 95 to ~ 135 nm in diameter. The polydispersity of the Pd-coated gold nanoparticles shown in Figure 1 likely arises in part from the polydispersity/inhomogeneity of the gold nanoparticle cores.

In contrast, the surfaces of the Pd-coated silica nanoparticles appear smooth and homogeneous, regardless of the size (Figure 2). When holding the concentration of the palladium salt solution constant but systematically decreasing the amount of silica-core particles (~ 100 nm in diameter), the size of the Pd-coated silica particles systematically increases, which indicates that the thickness of the palladium shells can be precisely controlled. We note that a trace amount of smaller particles (~ 10 nm in diameter) are produced concomitantly with the Pd-coated silica nanoparticles; we infer that these particles are Pd-coated gold nanoparticles, which arise from THPC gold seeds that detach from the silica cores during the coating process.

Figure 3, panels b–d, show large silica nanoparticle cores (~ 500 nm diameter) coated with varying palladium shell thicknesses (20–60 nm). In contrast to the smaller silica cores (100 nm in diameter) where it is possible to grow shells as thin as ~ 10 nm (see Figure 2b), we had difficulty growing shells thinner than 20 nm on the large silica cores. Palladium

(48) Pham, T.; Jackson, J. B.; Halas, N. J.; Lee, T. R. *Langmuir* **2002**, *18*, 4915.

(49) We note that the operative mechanism(s) here might be entirely distinct from those elucidated in pulse radiolysis studies, such as those in described in refs 19, 22, and 50.

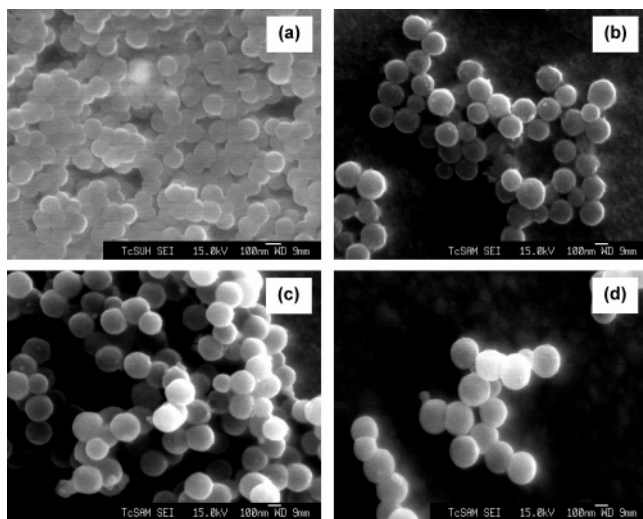


Figure 2. FE-SEM images of (a) THPC gold-attached silica cores ~ 100 nm in diameter and the same cores with Pd shells having thicknesses of (b) ~ 10 nm, (c) ~ 20 nm, and (d) ~ 30 nm.

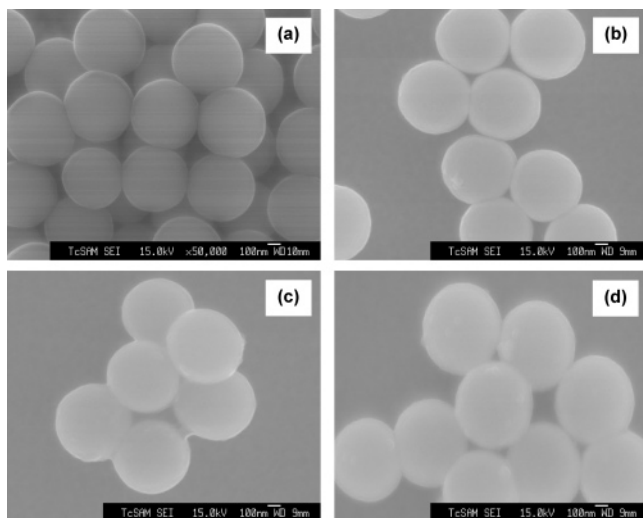


Figure 3. FE-SEM images of (a) THPC gold-attached silica cores ~ 500 nm in diameter and the same cores with Pd shells having thicknesses of (b) ~ 20 nm, (c) ~ 40 nm, and (d) ~ 60 nm.

coatings thicker than 20 nm were, however, reproducibly generated without failure.

The TEM images in Figures 4 and 5 clearly demonstrate the coating of palladium shells onto gold- and silica-core particles. The surface of the Pd-coated particles is noticeably rougher than that of the bare core particles. Moreover, the particles with gold cores possess rougher morphologies with broader size distributions than those with silica cores. We believe that these differences arise due to the fact that the surface of the gold cores is rougher than that of the silica cores. In addition, any crystalline structures corresponding to bare gold nanoparticles (Figure 4a) are undetectable in the images of the palladium-coated (Figure 4b–4d).

We performed EDX measurements to characterize the elemental composition of the particles. Figure 6 shows intense palladium peaks ($L\alpha$, $L\beta$ at 2.85 keV), indicating the deposition of palladium onto the gold and silica surfaces. Weaker peaks for gold ($M\alpha$ at 2.12 keV) and silica ($K\alpha$, $K\beta$ at 1.75 keV) are also observed in Figure 6, panels a and b, respectively. We note that the intensities of the palladium

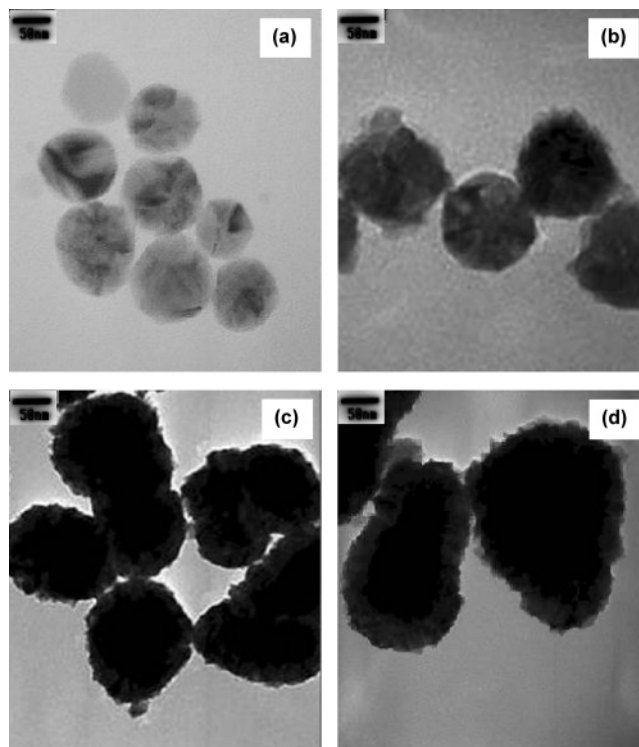


Figure 4. TEM images of (a) bare gold nanoparticle cores ~ 75 nm in diameter and the same cores with Pd shells having thicknesses of (b) ~ 10 nm, (c) ~ 20 nm, and (d) ~ 30 nm.

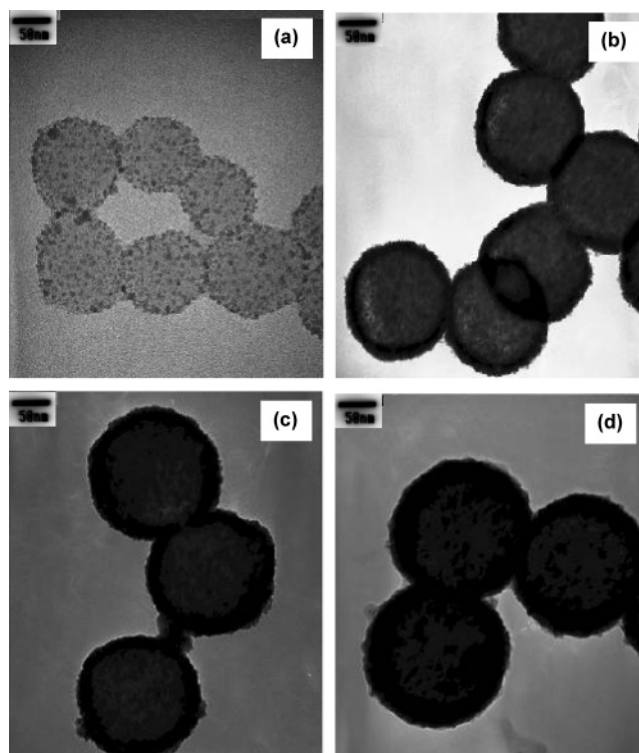


Figure 5. TEM images of (a) THPC gold-attached silica cores ~ 100 nm in diameter and the same cores with Pd shells having thicknesses of (b) ~ 10 nm, (c) ~ 20 nm, and (d) ~ 30 nm.

signals are stronger than those of gold or silica perhaps because the bulk of the shell materials are composed of palladium (i.e., it is possible that palladium shell attenuates the signals arising from the core materials). In general, EDX is not a surface analysis technique because the X-rays can

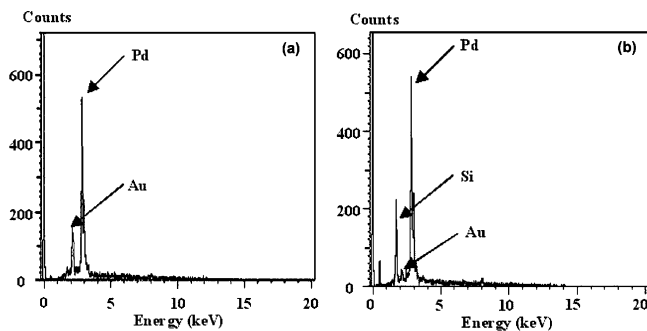


Figure 6. EDX spectra of (a) Pd-coated gold nanoparticle cores and (b) Pd-coated silica nanoparticle cores.

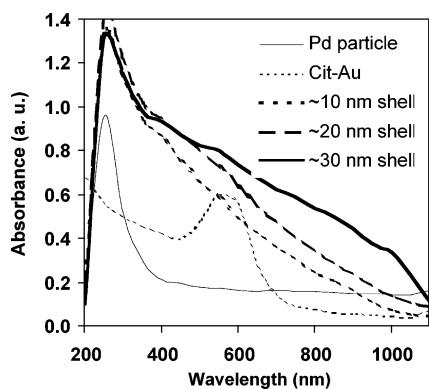


Figure 7. UV-vis spectra of Pd nanoparticles, citrate gold nanoparticles, and Pd-coated gold nanoparticle cores. For the latter samples, the particle concentration was adjusted such that the initial citrate gold solution exhibited 0.6 au at 560 nm.

penetrate as deep as $2 \mu\text{m}$.⁵¹ Consequently, we would not expect to observe EDX spectra of shell/core nanoparticles in which the core materials are absent.

Figure 7 shows the UV-vis spectra of small palladium nanoparticles, citrate-reduced gold nanoparticles, and Pd-coated gold nanoparticles. The broad absorption band with a λ_{max} at ~ 230 nm is characteristic of bare palladium nanoparticles less than 10 nm in diameter,⁵⁰ and that at 560 nm is characteristic of citrate reduced-gold nanoparticles ~ 75 nm in diameter.⁵² The absorption bands of Pd(II) in acidic solution appear at 350–450 nm (data not shown), which is consistent with the reported spectrum.⁵³ This band disappears completely as soon as the palladium shell forms. In addition, the absorption bands in the visible region increase in intensity and broaden upon formation of the palladium shell. In general, the absorption is enhanced at all visible and near-IR wavelengths up to ~ 1000 nm. The absorption properties of these relatively large Pd-coated gold nanoparticles are consistent with those of smaller Pd-coated gold nanoparticles described previously.^{22,50} These data therefore collectively confirm the formation of composite nanoparticles having gold cores coated with palladium shells.⁵⁴

Figure 8 shows the UV-vis spectra of bare silica-core particles, THPC gold seeds on the silica cores, and Pd-coated silica nanoparticles having various shell thicknesses and core sizes. In Figure 8a, the gold-seeded nanoparticles give rise

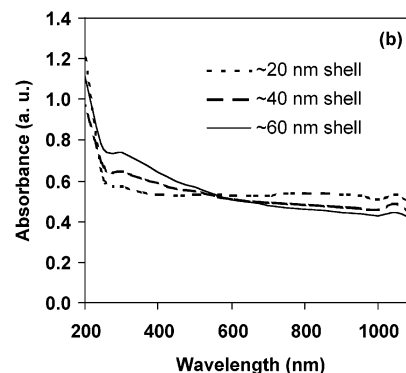
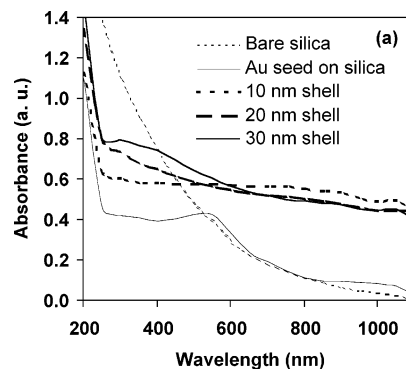


Figure 8. UV-vis spectra of Pd-coated silica nanoparticle cores (a) ~ 100 nm in diameter and (b) ~ 500 nm in diameter. The concentration of Pd nanoshells can be estimated from the initial number of silica particles in solution: (a) $\sim 7 \times 10^{10}$ particles/mL and (b) $\sim 6 \times 10^8$ particles/mL.⁴⁸

to a weak plasmon band at 520 nm, which is shifted to ~ 10 nm longer wavelength than that of free THPC gold nanoparticles (data not shown). The observed red shift is likely due to colloidal aggregation on the surface of the silica particles.²⁹ We note that the spectrum of the THPC gold seed-attached silica nanoparticles presented here is consistent with that reported in a previous study in which the authors attributed the red shift to a collective effect arising from the presence of gold nanoparticle clusters on the surface of the silica-core particles.⁴³

Upon shell formation, Figure 8 shows that the peaks for the palladium salt solution and the Au seed-coated silica particles disappear, and the absorption broadens across a wide range of wavelengths (~ 300 – 1000 nm). Although the broad absorption appears to be largely independent of the thickness of the shells, we note that the bands exhibit enhanced intensities with increasing thickness at wavelengths < 500 nm, but diminished intensities with increasing thickness at wavelengths > 500 nm. We note further that the absorption intensities of the Pd-coated silica nanoparticles are stronger in the visible and near-IR region compared to those of the Pd-coated gold nanoparticles (see Figure 7). This difference probably arises from the differing dielectric constants of the cores.⁵⁵ We also compared the UV-vis spectra of the Pd-coated gold and silica nanoparticles to those of calculated spectra based on Mie theory for multilayer particles (see

(50) Henglein, A. J. *Phys. Chem. B* **2000**, *104*, 6683 and references therein.

(51) Laskin, A.; Cowin, J. P. *Anal. Chem.* **2001**, *73*, 1023.

(52) Link, S.; El-Sayed, M. A. *J. Phys. Chem. B* **1999**, *103*, 4212.

(53) Nath, S.; Praharaj, S.; Panigrahi, S.; Ghosh, S. K.; Kundu, S.; Basu, S.; Pal, T. *Langmuir* **2005**, *21*, 10405.

(54) We note that separate studies utilizing galvanic replacement of Ag with Pd afforded ~ 50 nm diameter Pd-Ag “nanoboxes” that also exhibited strongly red-shifted absorptions: Chen, J.; Wiley, B.; McLellan, J.; Xiong, Y.; Li, Z.-Y.; Xia, Y. *Nano Lett.* **2005**, *5*, 2058.

(55) Grady, N. K.; Halas, N. J.; Nordlander, P. *Chem. Phys. Lett.* **2004**, *399*, 167.

Supporting Information).⁵⁶ The calculated UV–vis spectra generally correspond to the experimental UV–vis spectra except at wavelengths ≤ 300 nm. At present, we do not understand the origin of the latter discrepancy.

As a whole, these studies demonstrate that the reduction of palladium salts in the presence of gold-seeded silica nanoparticle cores enables the formation of Pd-coated nanoparticles having a wide range of core sizes (75–500 nm) and palladium shell thicknesses (10–60 nm). The dimensions of these composite particles are substantially larger than any previously reported Pd-based nanoparticles or nanocomposite particles. Furthermore, our studies have found that the use of gold-seeded silica nanoparticle cores affords greater control over nanoparticle dimensions when compared to the direct growth of palladium shells on gold nanoparticle cores.

Conclusions

This report demonstrates the growth of palladium shells on the surfaces of conducting gold and dielectric silica nanoparticle cores. The methods described herein enable the synthesis of core–shell particles having dimensions substantially greater than 50 nm in diameter. Monodispersed particles (silica and gold) with various core sizes (75–500 nm) and controllable palladium shell thicknesses (10–60 nm)

were obtained by using L-ascorbic acid for the reduction of PdCl₂ solution on citrate-stabilized gold (~75 nm) or THPC gold-attached silica particles (100–500 nm). All of the analyses collectively confirm the formation of Pd-coated gold and silica nanoparticles in sizes ranging from ~100 to 600 nm in overall diameter without requiring the use of external stabilizers. UV–vis measurements show that palladium nanoshells with gold cores have more intense red-shifted absorptions than those with silica cores. Future studies will explore the use of these materials in catalysis and the use of SAM technology to enhance their incorporation into various supporting media for device applications.

Acknowledgment. We gratefully acknowledge financial support from the Army Research Office, the National Science Foundation (ECS-0404308), and the Robert A. Welch Foundation (Grant E-1320). The use of the DLS was made possible by a grant from the Department of Energy to Professor Simon Moss (UH). We also thank Dr. James K. Meen (UH) for assistance with the FE-SEM and EDX measurements, Dr. Irene A. Rusakova (UH) for assistance with the TEM measurements, and Dr. Joseph B. Jackson (Nanospectra Biosciences) for calculating the UV–vis spectra.

Supporting Information Available: Comparison of experimental and calculated UV–vis spectra of Pd-coated gold and silica nanoparticles. This material is available free of charge via the Internet at <http://pubs.acs.org>.

(56) Mie, G. *Ann. Phys.* **1908**, 25, 377.